Ultracold neutrons: Their role in studies of condensed matter

R. Golub

Hahn Meitner Institut, 14109 Berlin, Germany

Ultracold neutrons, that is, neutrons whose energy is so low that they can be contained for long periods of time in material and magnetic bottles, provide the basis for the currently most sensitive experiments seeking to detect the neutron electric dipole moment and to measure the neutron lifetime. The goal of this article is to review the work that has been done to date in applying ultracold neutrons to the study of condensed matter and to discuss the future prospects for this type of research. [S0034-6861(96)00202-4]

CONTENTS

I. INTRODUCTION

Until the early seventies free neutrons could be studied only under conditions in which they spent no more than a brief moment within the experimental apparatus. Even "long-wavelength" neutrons with $\lambda \sim 10$ Å, $v \sim 400$ m/s take only 2.5 ms to travel 1 m. When diffusing through matter, neutrons have average lifetimes of, for example, 0.2 ms (H_2O) or 130 ms (D_2O). However, the development, since the midseventies, of ultracold neutron (UCN) technology has now reached the point where neutrons can be stored in material and magnetic bottles, for times that are essentially limited by the neutron's β-decay lifetime ($\tau_\beta \sim 900$ s) (Mampe *et al.* 1989a, 1989b). This has opened up the possibility of a wide range of new applications, some of which have reached a comparatively advanced stage of development while others are only taking their first tentative steps.

The UCN applications that have shown the greatest success to date are those relating to the fundamental properties of the neutron: the search for the time-reversal violating electric dipole moment of the neutron and the most accurate measurement of the neutron β decay lifetime. Pendlebury (1993) gives a review of the current situation with detailed references.

In the present article we should like to address the issue of the application of ultracold neutrons to studies of condensed matter. In comparison with the applications mentioned above, the use of UCN scattering as a tool to study condensed matter is still in its infancy. We shall review what has already been done in this field and give a few pointers to possible future developments.

In order to be totally reflected at all angles of incidence from an appropriate surface, and hence to have the ability to be stored for long periods of time, neutrons must have a velocity of the order of 5 m/s. Although this is very small in comparison to typical velocities of neutrons thermalized at room temperature ($v \sim 2200$ m/s), or even at the temperature of a liquid hydrogen or deuterium cold source ($v \sim 700$ m/s) all UCN sources to date have operated by extracting neutrons from the low energy tail of the distribution in the source. The strongest existing source is the source installed at the Institut Laue-Langevin (ILL) in Grenoble (Steyerl *et al.*, 1986; Steyerl and Malik, 1989). Other sources currently in operation and the prospects for improved sources have been discussed by Golub *et al.* (1991). (See also Sec. VII.B and Serebrov *et al.*, 1994.)

The phenomenon of total reflection of neutrons at grazing incidence, first demonstrated experimentally by Fermi and Zinn (1946) and by Fermi and Marshall (1947), has found extensive application in the construction of neutron guide tubes (Maier-Leibnitz and Springer, 1963) at many installations around the world.

A. Short history of ultracold neutron research

It is customary to denote as ultracold neutrons those neutrons having total energies

$$E < V = \frac{2\pi\hbar^2}{m} \sum_i N_i a_i \pm \vec{\mu} \cdot \vec{B}, \tag{1}$$

where N_i is the number density of nuclei of species i in the material, a_i is the coherent scattering length of a species i nucleus, and V is the effective potential for the neutrons in the medium. In practical units

$$V = 157 \rho_{g/\mathrm{cm}^3} a_{\mathrm{fermis}}/A \pm 6.03 B_{\mathrm{kilogauss}}(\mathrm{neV}), \tag{2}$$

where ρ_{g/cm^3} denotes the density, measured in g/cm^3, and A the atomic mass of the element in the medium; a is measured in fm and B in kG.

The idea that these neutrons will be totally reflected for any angle of incidence and, as a result, could be stored in closed containers has been attributed by many people to Fermi himself. However, the first person to take the idea seriously enough to put it into print was Zeldovitch (1959) who discussed the possibility of UCN storage in a graphite bottle and estimated the storage time due to absorption in the walls as well as the UCN densities to be expected. Zeldovich estimated that a thermal neutron flux of 10^{12} n/cm^2/s cooled to 3 K in liquid helium would produce a UCN density of 50 cm^{-3}. It is interesting to note that such densities have now been achieved at the Institut Laue-Langevin, Grenoble, using a reactor with a thermal flux of 10^{15} n/cm^2/s cooled to 20 K in a deuterium-filled cold source. Zeldovich suggested it would be interesting to study the interactions of the stored ultracold neutrons with substances introduced into the cavity, such as (n,γ) absorbers.

This work was followed by several other proposals. Vladimirskii (1961) suggested the use of inhomogeneous magnetic field gradients for confining ultracold neutrons. He also suggested extraction of ultracold neutrons from a reactor core by means of a vertical channel and pointed out the widening in solid angle as the neutrons travel up the guide. He noted that the effects of the moderator potential on the energy distribution of the ultracold neutrons leaving the moderator could be eliminated by vertical extraction.

Doroshkevich (1962) suggested beryllium as a storage material and discussed the temperature dependence of the loss rate.

Foldy (1966) suggested the use of liquid helium ($V=1.1\times10^{-8}$ eV) as a wall-coating material for a UCN bottle. However, this potential is rather low compared to those achieved with other materials ($V\gtrsim10^{-7}$ eV).

In 1966 Maier-Leibnitz published some remarks concerning the utility of slow neutrons for measuring neutron scattering at low values of ω and Q (see the appendix). Shortly afterwards, in 1968, Shapiro published a review article on the electric dipole moment of elementary particles. In this article he pointed out the advantages of ultracold neutrons in the search for a neutron electric dipole moment, in particular the greatly increased observation time and the reduction of the "$\mathbf{v}\times\mathbf{E}$" effect (a magnetic field, produced in the frame of the moving neutron by the applied electric field, interacts with the neutron's magnetic moment, imitating an electric dipole moment). See also Golub and Pendlebury (1972) for a more detailed discussion of this point. These two rather different observations were to provide the main motivations for the development of UCN research.

Given that the energy V, Eqs. (1) and (2), is some 10^5 times smaller than the thermal energy of neutrons in the reactor moderator, and the Maxwellian energy spectrum for neutron flux is proportional to E for low energies, it is remarkable that two groups, independently, had the courage to invest the time and effort to construct the necessary installations in the hope that neutrons so far from the peak of the Maxwell distribution did indeed exist inside the reactor, and that they could be extracted without crippling losses of intensity. That both groups, at Dubna and Munich, were successful almost simultaneously is one of those coincidences which seem to be so common in the history of physics. As was already noted, the motivations of the two groups were somewhat different, the Dubna group following the lead of Shapiro's article on electric dipole moments, while the Munich group seems to have been more interested in pioneering the sorts of UCN applications to condensed-matter studies that will be the main subject of this review.

The Dubna group under Shapiro (Luschikov *et al.*, 1968, 1969) extracted ultracold neutrons from a very low-power pulsed reactor by means of a curved horizontal channel 9.4 cm inner diameter and 10.5 m long. Counting rates of 0.8 counts per 10^2 s (background $\sim$0.4 counts per 10^2 s) were obtained. By admitting a gas of ^{4}He to the extraction pipe the authors attempted to estimate the storage time in the pipe. The idea is that when the average lifetime of a neutron for collisions with the helium

$$\tau_{\mathrm{He}}=[N_{\mathrm{He}}\sigma_{\mathrm{He}}\bar{v}_{\mathrm{He}}]^{-1} \tag{3}$$

is equal to the average lifetime for wall losses the counting rate should be reduced by 1/2 with respect to that in the absence of helium. This first attempt to measure storage times gave a result of 200 s, which is to be compared to 12 s obtained later from more detailed measurements (Groshev *et al.*, 1971), the discrepancy being attributable to possible impurities in the helium.

Working at Munich, Steyerl (1969) obtained ultracold neutrons by vertical extraction from a steady-state reactor. The beam was pulsed by a rotating chopper constructed out of 13 boron silicate glass plates located deep within the reactor swimming pool two meters above the core, allowing time-of-flight measurements of neutron spectra. The counting rate showed a steep drop below 10 m/s, probably due to absorption in the aluminum windows, to reflection losses, and to the limited acceptance angle of the detector. However, total cross sections were measured for neutron velocities down to 7 m/s for gold and 5 m/s for aluminum.

It is noteworthy that both of these initial attempts were made with relatively low-intensity sources (an average thermal flux of 1.6×10^{10} n/cm^2/s in the Dubna experiment and 10^{13} n/cm^2/s in the Munich experiment), thus demonstrating the possibility of making important innovations with weak sources.

Following these first experiments, Okun (1969) called attention to Shapiro's point that ultracold neutrons offered a promising method for improving the sensitivity of the search for a neutron electric dipole moment, emphasizing the potential improvement in observation times—10^3 s for ultracold neutrons, compared to 10^{-2} s in a typical beam experiment. He also pointed out the potential of ultracold neutrons for measuring the neutron lifetime.

The neutron lifetime is less well known than that of the μ and π mesons. This is because the neutrality of the neutron means that its trajectories cannot be measured by ionization—the only way to detect a slow neutron is to have it absorbed into a nucleus. Thus to determine the neutron lifetime in a beam experiment it is necessary to know the absolute efficiencies of both a neutron detector and of the charged-particle detector used to detect one of the decay products (proton or electron). With stored ultracold neutrons, the measurements can be carried out with a single detector, either for the neutrons or the decay products. However, with stored neutrons one must be sure that there are no processes, other than β decay, which can result in ultracold neutrons leaving the storage vessel. For example, wall losses must be kept to a minimum or be very well understood. See Erozolimskii (1975) for an early review of this topic, as well as the series of papers dealing with the neutron lifetime in Dubbers, Mampe, and Schreckenbach (1989), for example, Erozolimskii, 1989; Mampe *et al.*, 1989a, 1989b. The possibility of using the decays of polarized ultracold neutrons to study parity and time-reversal violation in neutron β decay has not yet been explored.

Both of these fundamental physics applications of ultracold neutrons [EDM (see Smith *et al.*, 1990) and neutron lifetime] have now achieved a first level of success, reporting results considerably more precise than those achieved with classical neutron-beam methods. The reader is invited to look back over the series of conferences concerned with the fundamental physics of reactor neutrons (von Egidy, 1978; Desplanques *et al.*, 1984; Greene, 1986; Dubbers *et al.*, 1989) to see the fascinating development of the application of ultracold neutrons to these questions.

The field of UCN research has expanded considerably since this pioneering work and there are now a number of books and review articles available covering ultracold neutrons in more detail than is possible in this short review (Steyerl, 1977; Golub and Pendlebury, 1979; Ignatovich, 1986; Golub *et al.*, 1991; Pendlebury, 1993).

B. Ultracold neutrons and condensed matter

Ultracold neutrons can be used to study condensed matter in several ways. These include (i) reflection and tunneling studies (UCN reflectometry), (ii) elastic scattering, (iii) quasielastic or inelastic scattering, and (iv) upscattering. By upscattering we mean inelastic scattering with energy transfer $\hbar\omega \gg E_{\rm UCN}$, the UCN energy, while by inelastic scattering we refer to scattering with $\hbar\omega \sim E_{\rm UCN}$ and by quasielastic scattering to the case with $\hbar\omega \ll E_{\rm UCN}$.

One of the original motivations for UCN research was the fact, first noted by Maier-Leibnitz (1966), that for an inelastic-scattering experiment at a given Q (=momentum transfer) with $\hbar\omega \ll E_i, Q < k_i$, one can always gain intensity by going to lower incident energy. If the entire phase space allowed by the requirements on ω and Q can be used, the intensity will grow as $1/E_i$ as the incident energy is reduced (see also Golub *et al.*, 1991 and the Appendix).

We now turn to a discussion of the application of the interactions of ultracold neutrons with condensed matter, beginning with reflection and tunneling studies.

II. REFLECTION AND TUNNELING FROM SURFACES AND MORE COMPLEX STRUCTURES

The interaction of ultracold neutrons with materials can most usefully be characterized by the interaction potential

$$U = V - iW \tag{4}$$

where V is given by Eq. (1), and

$$W = \frac{\hbar}{2}\sum_i N_i \sigma_l^{(i)} v = 3.3\times 10^{-7} N_{10^{22}/\mathrm{cm}^3} \sigma_{l,\mathrm{barns}} v_{\mathrm{m/s}}(\mathrm{neV}), \tag{5}$$

where $\sigma_l^{(i)}$ is the loss (absorption plus inelastic scattering) cross section for species i, with number density N_i; the units in which quantities are to be measured are denoted by subscripts. In general $\sigma_l^{(i)} v$—and hence W—is independent of neutron velocity v.

For absorbing materials the wave function can be calculated by standard methods, neglecting W and the absorption, and then substituting Eq. (4) for V in the resulting expression for the reflection coefficient R. Alternatively, for weak absorbers, one can use the wave function obtained with $W=0$ to calculate the absorption probability per bounce, P_l, according to Lanford and Golub (1977):

$$P_l = \int [N\sigma_l(v)]_x |\psi(x)|^2 dx, \tag{6}$$

with ψ normalized to an incident wave e^{ikx}:

$$\psi(x) = e_{ikx} + Re^{-ikx}. \tag{7}$$

We see that $P_l = \tau_D/\tau_l$, where

$$\tau_l = [N\sigma_l(v)v]^{-1} \tag{8}$$

is the absorption time in a locally uniform medium and

$$\tau_D = \frac{1}{v}\int_\Omega |\psi(x)|^2 dx \tag{9}$$

is the dwell time of neutrons in the region Ω (assuming the absorption is weak enough so as not to significantly change the wave function). Thus doping with known amounts of absorber can serve as a method of measuring the dwell time in UCN tunneling (Hauge and Stø vneng, 1989; Golub *et al.*, 1990) and has been proposed as a method for measuring the phase of the reflection coefficient R in Eq. (7) (Fiedeldey *et al.*, 1992).

Matrix methods are used for calculating the reflection from more complicated layered surfaces. As the wave function inside a layer consists of two independent (complex) functions, we use 2×2 (complex) matrices. These matrices can be based on the values of $\psi(x)$ and $\psi' = d\psi/dx$, or on the amplitudes of the forward ($\sim e^{ikx}$) and backward ($\sim e^{-ikx}$) traveling waves in a

layer (Lekner, 1987). Taking the particles as incident from the left and numbering the layers with numbers increasing to the right (i.e., to greater depths) we proceed according to the latter representation by writing the wave function in the nth layer as

$$\psi_n(z)=A_n e^{ik_n z}+B_n e^{-ik_n z} \tag{10}$$

where $k_n=\sqrt{(2m/\hbar^2)(E-U_n)}$ may be complex (see also Penfold and Thomas, 1990).

Applying the usual boundary conditions, we obtain

$$\begin{pmatrix} A_n \\ B_n \end{pmatrix}=\frac{1}{2}\begin{bmatrix} (1+\gamma_n)e^{i(k_{n-1}-k_n)z_n} & (1-\gamma_n)e^{-i(k_{n-1}+k_n)z_n} \\ (1-\gamma_n)e^{i(k_{n-1}+k_n)z_n} & (1+\gamma_n)e^{-i(k_{n-1}-k_n)z_n} \end{bmatrix}\begin{pmatrix} A_{n-1} \\ B_{n-1} \end{pmatrix} \tag{11}$$

$$\equiv \bar{M}_n\begin{pmatrix} A_{n-1} \\ B_{n-1} \end{pmatrix}, \tag{12}$$

with $\gamma_n=k_{n-1}/k_n$.

For an incident wave given by Eq. (7) we have

$$\begin{pmatrix} A_o \\ B_o \end{pmatrix}=\begin{pmatrix} 1 \\ R \end{pmatrix}, \tag{13}$$

and thus

$$\begin{pmatrix} T \\ 0 \end{pmatrix}=\bar{M}\begin{pmatrix} 1 \\ R \end{pmatrix}, \tag{14}$$

with

$$\bar{M}=\bar{M}_N\cdots\bar{M}_2\bar{M}_1=\begin{pmatrix} \bar{M}_{11} & \bar{M}_{12} \\ \bar{M}_{21} & \bar{M}_{22} \end{pmatrix}. \tag{15}$$

Then

$$\det\bar{M}=\frac{k_1}{k_2}, \tag{16}$$

and

$$R=\frac{-\bar{M}_{21}}{\bar{M}_{22}}, \quad T=\frac{k_1/k_2}{\bar{M}_{22}}. \tag{17}$$

The UCN diffractometer designed and constructed by Steyerl and co-workers (Scheckenhofer and Steyerl, 1977, 1981; Steyerl *et al.*, 1981) employs the Earth's gravitational field to define the vertical component of velocity for neutrons incident on, and reflected or diffracted by a sample.

The principle is shown in Fig. 1. The incident neutrons are constrained to be moving horizontally by the entrance slits, so the incident vertical velocity is determined by the height difference between these slits and the sample. The final vertical velocity is determined by the height of the exit slit with respect to the sample. Samples for diffraction experiments are placed at the position shown for ruled gratings while reflection samples are placed in the horizontal mirror position. The diffractometer accepts a wide band of horizontal UCN velocity components (average $\sim$4 m/s) while accurately defining and analyzing the vertical component.

In Fig. 2 we see the results of UCN reflectivity measurements made on a mirror of borosilicate glass (Scheckenhofer and Steyerl, 1977). This is clear evidence that the potential-step model does not hold for the surface of the sample used, the data fitting much better to a potential given by

$$V(z)=V_o/(1+e^{-z/d}), \tag{18}$$

as shown in inset (ii). While this behavior can be due to a depth-dependent density of the glass, a more likely explanation is the presence of surface hydrogen, which, with a scattering length of -3.74×10^{-12} cm will reduce the potential by an amount proportional to the local hydrogen density (see Golub *et al.*, 1991, for a detailed discussion of this point).

Transmission measurements can be made by placing the sample some distance (about 16 cm) above the horizontal mirror in the diffractometer. Figure 3 shows transmission measurements on the sample whose structure is shown in the inset. The resonances occur at energies corresponding to bound states in the potential well formed by the two barriers. The widths of the resonances are determined almost entirely by the lifetime of the bound states (Steinhauser *et al.*, 1980). The two resonances correspond to the first two excited states ($n=1$ and $n=2$).

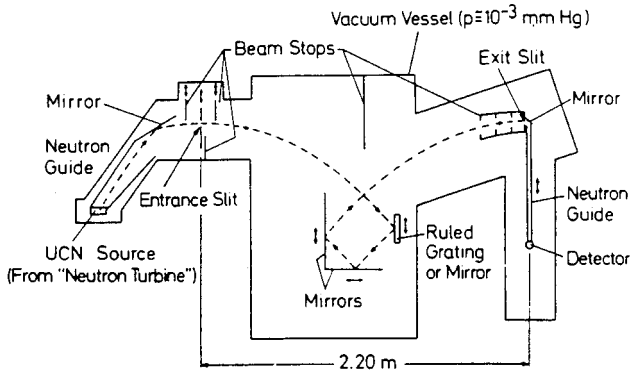

FIG. 1. Schematic view of the UCN gravitational diffractometer (Scheckenhofer and Steyerl, 1977).

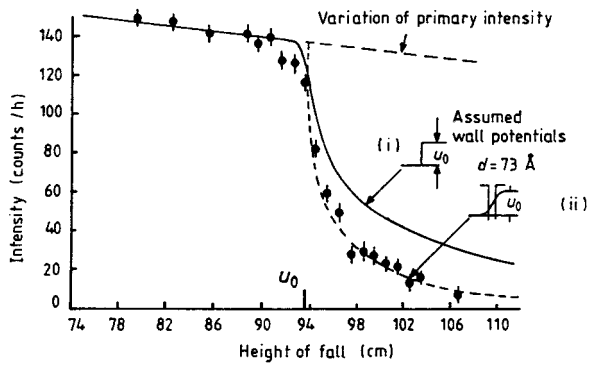

FIG. 2. The measured intensity reflected from a glass mirror (points) compared with theoretical curves for (i) a step function and (ii) a smoothed step function for the wall scattering potential: broken curve, calculation for monoenergetic neutrons; full curve, calculation for the instrumental resolution. Assumption (ii) may be a model for a hydrogenous surface contamination (Scheckenhofer and Steyerl, 1977).

In Fig. 4 we see the transmission as measured for the double-well potential. The $n=0$ level of the bound state is now split by tunneling through the central barrier, (Steyerl *et al.*, 1981). Steyerl *et al.* (1988) review these results and present some more recent results obtained with a blazed ruled grating at the ILL.

These experiments show how it is possible to bring a number of effects in one-dimensional quantum mechanics to life by combining thin-film technology with ultracold neutrons. Similar experiments can of course be performed with neutron reflectometry (Penfold and Thomas, 1990) and this has, in fact, been done (Steyerl *et al.*, 1981).

Perhaps the ultimate in complicated surfaces are the supermirrors (Mezei and Dagleish, 1977) which have been extensively studied by neutron reflectometry but not, to our knowledge, by UCN techniques.

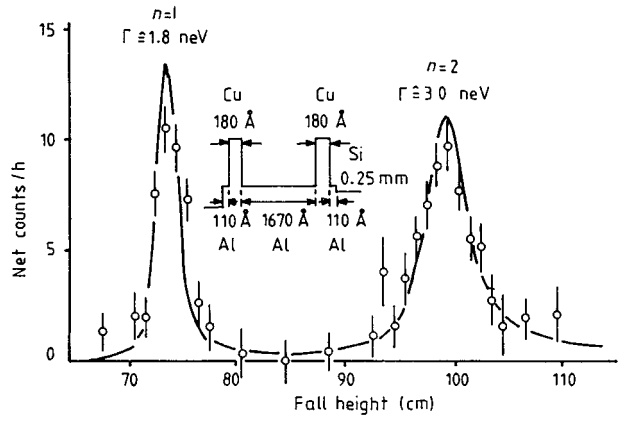

FIG. 3. Transmission data for a target with nominal layer thicknesses: Al (110 Å), Cu (180 Å), Al (1670 Å), Cu (180 Å), and Al (110 Å). The substrate is silicon 0.25 mm thick. The two resonances observed correspond to $n=1$ and $n=2$. The data are compared with the full curve calculated for a multistep potential (Steinhauser *et al.*, 1980).

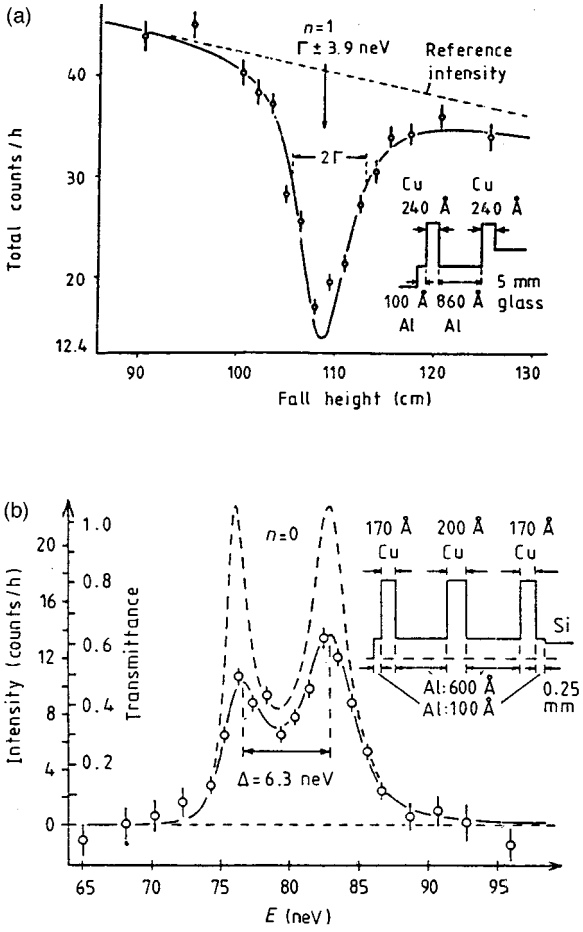

FIG. 4. Level splitting observed in UCN transmission through a sample with the indicated coupled-resonator structure (Steyerl *et al.*, 1988).

A. UCN reflectometry

As we have seen, the principles of UCN reflection are no different than those of reflection of cold or thermal neutrons. However, reflectometers using cold neutrons (Penfold and Thomas, 1990) are capable of measuring reflectivities approaching 10^{-6}, a value not attainable for UCN because of the much smaller available intensities. On the other hand, because of the high available normal energy resolution, ~ 0.5 neV for the UCN diffractometer shown in Fig. 1, a UCN reflectometer would be well adapted to measure the details of reflection near the critical energy.

Because of the Fourier-transform-like relation between reflection and potential, cold-neutron reflectometry, best suited to measurements at higher incident normal energies because of its ability to measure small reflection probabilities, yields most detailed information on the behavior of the potential near or underneath the surface. On the other hand, UCN reflectometry would be expected to yield more detailed information on the behavior of the potential far from the surface (Dietrich and Schack, 1987; Herrmann, 1990).

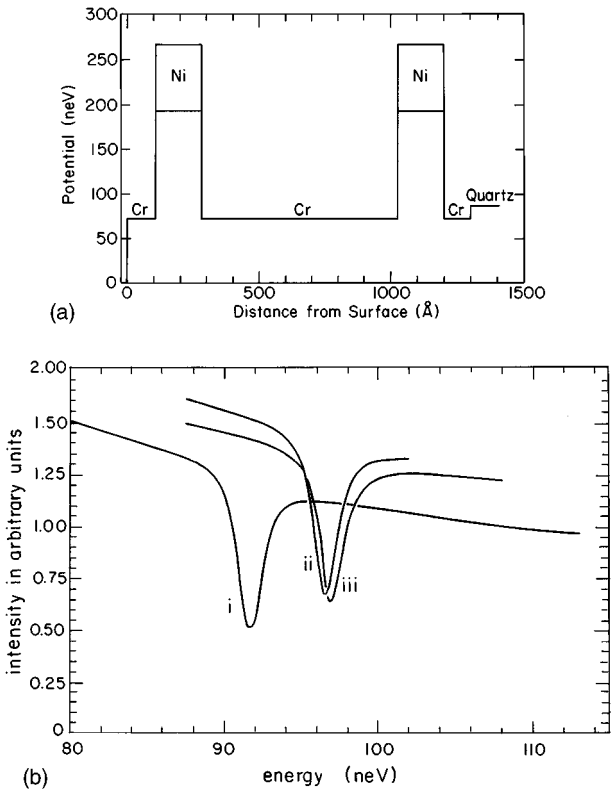

FIG. 5. Reflectivity of a multilayer structure. (a) Construction of a multilayer Fabry-Perot interferometer for ultracold neutrons; (b) UCN reflectivity of multilayer structure shown in Fig. 5(a): (i) Untreated sample; (ii) heat treatment 2h:25 at 360 °C; (iii) heat treatment 5h:05 at 360 °C. Solid curves: fit with two parameters. Vertical scale and displacement of (i) differs from the other curves (Herrmann, 1990).

Some initial steps in the development of UCN reflectometry have been taken by Gutsmiedl and Herrmann (Herrmann, 1990). They measured the reflectivity of the multilayer structure shown in Fig. 5(a). The results, shown in Fig. 5(b), represent (i) the reflectivity of the untreated sample, (ii) the sample after heat treatment of 2h:25 at 360 °C, and (iii) the sample after heat treatment of 5h:05 at 360 °C.

The measurements were fit to a simulation based on allowing the Ni in Fig. 5(a) to diffuse. The results of the fit gave a diffusion coefficient of $D=3\times10^{-17}$ cm^2/s for curve (ii), and $D=2\times10^{-17}$ cm^2/s for curve (iii). Note the shift in peak position from (ii) to (iii), while only $\sim$0.4 neV is clearly observable. The solid lines in Fig. 5(b) are the simulated fit curves. The only parameters used in the fit were a normalizing constant and the diffusion coefficient.

These results demonstrate the very exciting possibilities of UCN reflectometry. The apparatus has now been equipped with a polarizer, analyzer, and spin flipper, so that its field of application can be broadened to include magnetic structures.

III. ELASTIC SCATTERING

Because the early UCN sources were very weak, one looked for applications which were feasible with low

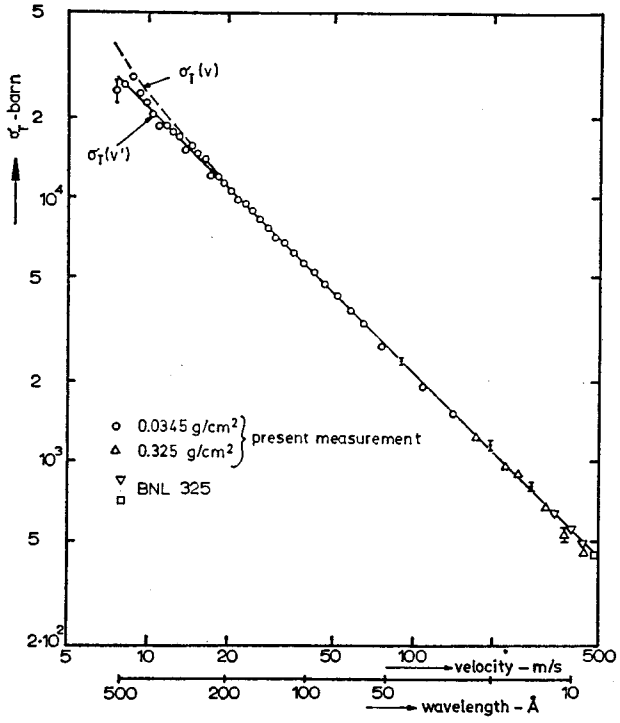

FIG. 6. Total cross section of two gold foils vs neutron velocity in vacua (v) and inside the sample (v'): at temperatures 80 and 299 K (Steyerl and Vonach, 1972).

counting rates. Steyerl and his co-workers carried out an intensive program of pioneering studies to demonstrate the usefulness of total-cross-section measurements for very-cold neutrons (VCN) and ultracold neutrons.

A. Scattering from homogeneous substances

As diffraction from crystals is impossible for neutrons with wavelengths $\lambda>2a$, where a is the largest lattice spacing in the crystal, the only effect of coherent elastic scattering is in the refraction discussed above. Absorption and inelastic-scattering cross sections are expected to vary as $1/v'$ where $v'=\sqrt{(2/m)(E-V)}$ is the velocity in the medium taking into account the potential energy (or index of refraction) in the medium (Landau and Lifshitz, 1958).

Because of this dependence, these processes will dominate the total cross section for very-cold neutrons. This could be useful for measuring absorption in rare isotopes, or generally for making high-accuracy measurements of absorption cross sections. The inelastic scattering is temperature dependent and the temperature dependence of the total cross section can yield information about the phonon spectrum. At low temperatures the inelastic scattering is negligible and we measure the absorption cross section. Steyerl and Vonach (1972) have measured the total cross section for gold, aluminum, copper, glass, mica, and air, using time of flight in a vertical extraction setup. Figure 6 shows the results for gold, plotted against v'. The dashed line shows what would be expected if the cross section depended on $1/v$.

By measuring the total cross section for Al at temperatures of 298, 95.5, and 33 K, the authors extracted a Debye temperature $\Theta = 389 \pm 50$ K, in reasonable agreement with other determinations.

The copper measurements showed some deviations from a $1/v'$ law, presumably due to inhomogeneities caused by the cold-rolling treatment given to the samples. Glass and air showed $1/v'$ dependences ($v' = v$ for air) while mica showed deviations.

Dilg and Mannhart (1973) reported a further set of similar measurements, confined to higher incident neutron energies where the difference between v and v' was not apparent. The results reported for the absorption cross sections of Sc, V, Cu, and Rh were accurate to about 0.5%.

B. Scattering from static inhomogeneities

Density inhomogeneities can contribute to the elastic scattering of ultracold neutrons. As was emphasized by Steyerl, the total elastic scattering cross section

$$\sigma(k) = \int d\Omega \frac{d\sigma}{d\Omega} = \int d\Omega S(Q) = \frac{2\pi a^2}{k^2} \int_0^{2k} S(Q) Q dQ \tag{19}$$

(the maximum momentum transfer from a neutron of momentum k is $Q = 2k$, i.e., backscattering) for small k contains the same information as $d\sigma/d\Omega \propto S(Q)$ for small angles (small Q). $S(Q)$ can, in principle, be recovered by differentiation of (19), but this is not necessary as the information can be recovered by an elegant technique (Lermer and Steyerl, 1976; Lengsfeld and Steyerl, 1977).

We will take scatterers in the form of solid spheres as a model. For $kR \gg 1$, where R is the radius of the spheres, the upper limit in Eq. (19) may be taken as infinite, the integral is then a constant and

$$\sigma(k) \propto \frac{1}{k^2}. \tag{20}$$

For higher k the angular size of the detector, θ_1, becomes important since those scatterings for which $Q < k\theta_1$ (inscattering), result in the scattered neutrons hitting the detector. Thus the lower limit of the integral in (19) should be replaced by $k\theta_1$.

When k is large enough that the inscattering includes all Q values except for the high-Q tail ($k\theta_1 \gg 1$)

$$\sigma(k) = \frac{1}{k^4}. \tag{21}$$

The intersection of the extrapolated behaviors [Eqs. (20) and (21)] can be shown to occur at

$$k_1 = \frac{1}{R\theta_1}. \tag{22}$$

Figure 7 shows the results (Lengsfeld and Steyerl, 1977) for a suspension of SiO_2 spheres of radius

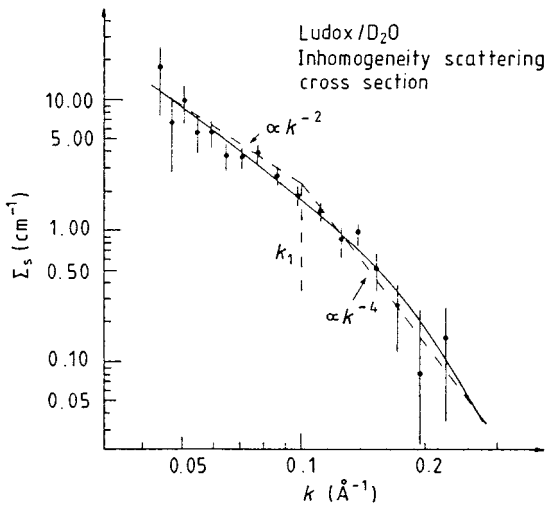

FIG. 7. Macroscopic cross section Σ for neutron scattering by the SiO_2 particles alone. The points, which were obtained from the measured data by subtracting $A + B/k$, are represented well by the full-fit curve of the form $C/k\ 2g(kr\theta_1)$. This function shows a k^{-2} behavior at small k and a k^{-4} asymptote at larger k (broken lines). The intersection point k_1 of the asymptotes is a convenient measure of the particle radius r (Lengsfeld and Steyerl, 1977).

$R = 65$–70 Å in a mixture of D_2O and $\sim 5\%$ H_2O, after correcting for the scattering of the liquid. The point is that we can determine the size of the scatterering particles from measurements of the *total cross section* alone.

Lermer and Steyerl (1976) have applied this technique to the study of ferromagnetic domains and domain walls. The analysis assumed that the domain walls were regions in the shape of discs of diameter $d \approx$ (domain size), and thickness t. While the analysis is complicated by the need to involve the coupling of the neutron spin to the magnetic field fluctuations [i.e., $a_{\text{coh}}\rho(\vec{r})$ is replaced by $-\vec{\mu}\cdot\vec{B}(\vec{r})$], the results are essentially the same. For both the domains and the walls, the low energy cross sections ($\sim 1/k^2$) go over to a $1/k^4$ dependence at higher incident k. In the case of the domains themselves the cross over value, k_1 [Eq. (22)], is determined by $R = d/2$, i.e., the domain size, while for the domain walls it is determined essentially by the wall thickness t. Figure 8(a) shows the measured cross section $\sigma(k)$ plotted against neutron velocity ($k = 1.59 \times 10^{-3}\ v_{\text{m/s}}$ Å^{-1}) for nickel. The scattering above the usual $1/v$ law is seen to vanish at $H \gtrsim 100$ G, indicating the disappearance of the domain walls as the material saturates. Figure 8(b) shows the $1/v^2$ and $1/v^4$ extrapolations for cobalt and the intersection point (v_o) of these extrapolations yielding $t = 225$ Å. From the size of the $1/k^4$ term it is possible to deduce that in cobalt the domain size $d = 3$ μm. Thus for the domains the break k_1 would come at a much lower neutron energy than that of the domain-wall scattering.

This technique is like the inverse of conventional small-angle scattering. At high k, the entire $S(Q)$ distri-

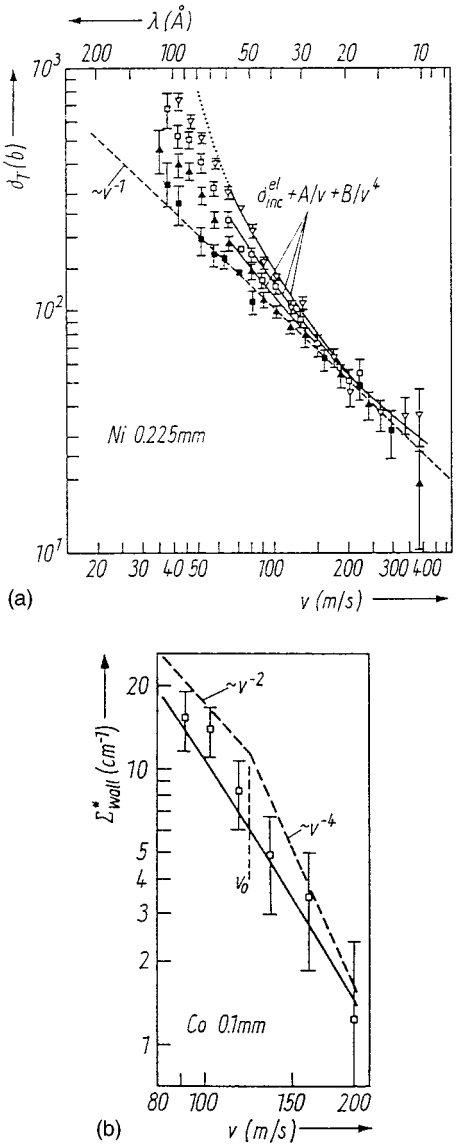

FIG. 8. Total cross sections for scattering and absorption: (a) Total experimental cross section σ_T per atom for nickel at different magnetic field strengths, plotted against the neutron velocity and wavelength (corrected for refraction within the sample). The $1/v$ contribution due to nuclear capture and thermal inelastic scattering (broken curve) is indicated. The full curves are fit curves taking account of incoherent elastic scattering ($\sigma_{\rm inc}^{\rm el}$), of absorption ($\sim 1/v$) and of the asymptotic behavior of scattering by Bloch walls and domains as a whole ($\sim v^{-4}$ at large v). In the range $v<v_o\approx 60$ m s^{-1} the data deviate noticeably from this higher-energy fit curve [which is extrapolated as a dotted curve for $H=0$ G (∇)]. The empty squares are for $H=30$ G; solid triangles 70 G; the full squares are for 100 G (Lermer and Steyerl, 1976); (b) Macroscopic scattering cross section of Bloch walls, $\Sigma^*_{\rm wall}$, in cobalt in the low-energy transition region from a v^{-4} to a v^{-2} variation. $\Sigma^*_{\rm wall}$ is obtained from the measured macroscopic cross section by subtracting the $1/v$ contribution due to absorption and a v^{-4} term corresponding to scattering by the domains as a whole. The full curve is a calculation for the transition region. The intersection point v_o of the v^{-4} and v^{-2} asymptotes (broken lines) is a measure of Bloch wall thickness (Lermer and Steyerl, 1976).

bution is concentrated at very small angles and scattered into the detector. As k decreases, the $S(Q)$ distribution spreads out to larger angles, the constant angle subtended by the detector acting as a window which rejects the larger Q values.

Following this pioneering work at a relatively weak source, this interesting technique has not yet been taken up at the more intense neutron sources, perhaps because the conventional small-angle scattering instruments are so well developed and there is more interest in developing the inelastic-scattering applications of ultracold neutrons (see below).

However, we should point out that the minimum Q available on a small-angle scattering instrument at the ILL, $Q_{\rm min}\approx 1\times 10^{-4}$ Å^{-1} (ILL, 1988) is reached at the relatively large angle of 10^{-2} radians for the 10 m/s neutrons, which are at the peak of the turbine output spectrum.

Binder (1971a, 1971b) has carried out a search for physical situations in which measurement of total cross sections for ultracold neutrons may be of interest. He suggested (i) the diffraction of ultracold neutrons from the periodic lattice formed by magnetic vortices in type-II superconductors, (ii) scattering from spin waves in ferromagnetic materials, and (iii) scattering from the fluctuations in a ferromagnet near the critical transition. In all cases he calculated the total cross section expected for ultracold neutrons.

The treatment of the spin waves is quite similar to the ordinary treatment of phonons, a major difference being that the spin waves (''magnons'') satisfy the dispersion relation

$$\omega=\omega_o+\alpha Q^2. \tag{23}$$

In the case of critical scattering one can (crudely) consider $S(Q,\omega)$ (proportional to the scattering cross section) as being made up of the Fourier transform of the spin correlation function

$$\langle \vec{S}_o\cdot\vec{S}_R\rangle \underset{R\to\infty}{\to} \frac{1}{R}e^{-R/R_o} \tag{24}$$

which Fourier transforms into

$$\chi(Q)\propto \frac{1}{Q^2+1/(R_o)^2}, \tag{25}$$

where the correlation length $R_o\to\infty$ as $T\to T_c$. For small energy transfers

$$S(Q,\omega)\sim\chi(Q)=\frac{\Gamma(Q)}{\omega^2+\Gamma^2(Q)}, \tag{26}$$

with

$$\Gamma(Q)=\Lambda Q^2 \quad \text{for } Q\ll 1/R_o \tag{27}$$

(Λ is called the spin-diffusion constant) going over to a faster Q dependence for $Q\gtrsim 1/R_o$. The total cross section at $v\lesssim 10$ m/s shows a rapid rise as $T\to T_c$.

IV. INELASTIC SCATTERING

It is possible to show, by an argument originally presented by Maier-Leibnitz (1966), that for a scattering

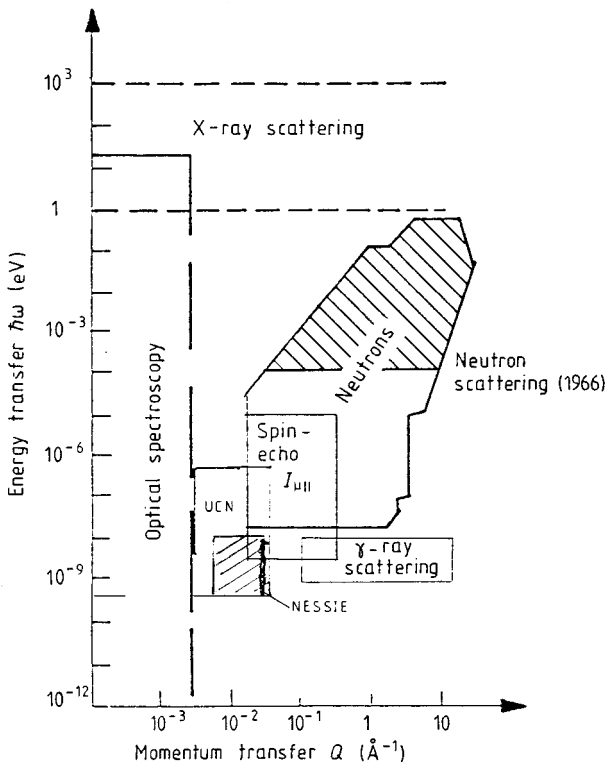

FIG. 9. Regions of ω-Q space accessible to different scattering techniques. Progress in neutron scattering since 1966 is indicated [after Egelstaff (1967)].

measurement at fixed $\vec{Q}$ (small compared to the incoming neutron $\vec{k}$), ω (small compared to the incoming neutron energy), and fixed $\Delta Q/Q$ and $\Delta\omega/\omega$ (the relative precisions of the Q and ω determinations), one can gain intensity $\propto \lambda^2$ by going to longer incident wavelengths, provided that one makes use of the entire phase space allowed by the desired ω, Q, $\Delta Q/Q$, and $\Delta\omega/\omega$ (see appendix). As a result of this we expect UCN scattering to be beneficial at relatively small values of Q and ω. Since coherent scattering by an object of size R, whose motions have a correlation time τ, is significant only for $QR \lesssim \pi$ and $\omega\tau \lesssim \pi$, we expect UCN scattering to be interesting for the study of slow motions of large objects and we are led to the domain of large molecules—polymers and biological molecules.

In Fig. 9 we show a by now well-known plot of ω-Q space. Such a plot was first introduced by Egelstaff (1967), and the shaded area shows the situation in neutron scattering at the time. The impressive improvement in neutron-scattering techniques since then is evident. The square labeled spin echo refers to an instrument developed by Mezei (1972) (see also Mezei, 1980), using the precession of the neutron spin in a magnetic field to measure the time of flight, and hence the velocity of the neutrons, before and after the scattering. A short description of this and many other neutron scattering instruments is given by Bée (1988). It is seen from the figure that UCN scattering is expected to fill the gap in Q between present neutron-scattering techniques and light-scattering techniques while taking the neutron-scattering techniques to lower values of ω. The only existing UCN scattering spectrometer, "NESSIE," at the ILL, operates over a limited Q region at $\sim 3\times 10^{-2}$ Å^{-1} in its present configuration. However, as we shall see below, this restriction can be easily overcome (Steyerl, 1978, 1992).

At present, there are several projects aimed at reducing the ω-Q limits of the spin-echo technique. There is an instrument at Saclay which is said to provide a factor-of-two improvement in both limits (Bée, 1988), and a project at the ILL which will work with 25 Å incident neutrons and which is expected to result in significantly lower Q values (ILL, 1988). In addition there is a new type of spin-echo technique (neutron resonance spin echo, NRSE) under development (Dubbers, El-Muzeini *et al.*, 1989; Keller *et al.*, 1990, 1995), which might provide some improvements over the existing technique. However at the moment the "NESSIE" instrument provides the best available ω resolution. One can also consider the possibility of a UCN spin echo based on the NRSE idea.

In addition to considering the accessible ω-Q region there are some other properties of neutron scattering which are useful to the study of large molecules. Coherent neutron scattering depends only on the variations of density (more precisely, the scattering length density) with respect to that of the surrounding medium. The coherent scattering length for protons (–3.74 fm) and deuterons (6.67 fm) are so different that mixtures of H_2O and D_2O (the scattering length of oxygen = 5.8 fm) covering a wide range of scattering length densities can be produced. Using this technique, combined with selective deuteration of different parts of a large molecule, one can adjust the relative scattering-length densities so that the neutron scattering takes place only from a determined section of a molecule. Different parts of a molecule can be separately studied.

However, there is a difficulty with the application of this technique to UCN scattering. Hydrogen has an incoherent cross section of 80 barns (1 barn$=10^{-24}$ cm^2) which is more than an order of magnitude larger than that of any other nucleus. Because of the kinematic factor (k_f/k_i), the scattering cross section for a given $\omega \sim k_B T$ will be much larger for ultracold neutrons than for faster neutrons, and the first UCN experiments were made only with solutions in pure D_2O. This incoherent scattering of ultracold neutrons at relatively large ω can swamp the desired low-ω coherent scattering. The problem requires further detailed study.

Incoherent scattering is also a problem for conventional small-angle scattering. In order to overcome this Nierhaus *et al.*, (1982) [see also Stuhrmann (1982) and May (1982)] developed a technique where an entire biological molecule (in this case a ribosomal subunit of Coli) can be contrast matched with a pure D_2O solution, thus eliminating the incoherent scattering from the protons in the solvent. The part of the molecule that one desires to study, such as a protein, can be replaced with

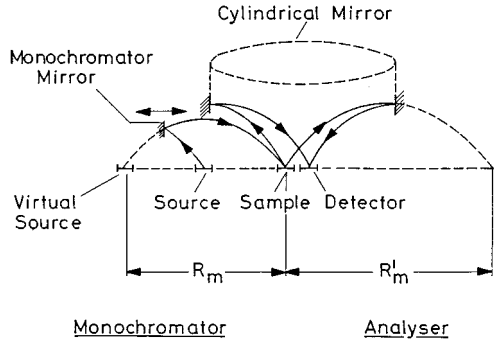

FIG. 10. Simplified scheme of a gravity spectrometer where the maximum reach of the flight parabolas followed by ultracold neutrons in the gravitational field is used for high-resolution energy analysis. The incident energy may be varied by displacement of the monochromator mirror, which results in a variation of the effective reach R_m. In the analyzer, neutrons leaving the sample with an energy corresponding to the reach R'_m are focused on the detector by a cylindrical mirror of slightly elliptical shape (Steyerl, 1978).

a natural (protonated) protein, allowing measurements to be made on very dilute solutions. The possible application of this technique to UCN scattering remains an open question.

The only operating UCN spectrometer, "NESSIE," works on the principle of "reach analysis" (Steyerl, 1978; Steyerl *et al.*, 1983). This is based on the observation that the maximum distance traveled by a particle following a parabolic trajectory in the Earth's gravitational field is proportional to the particle's energy. For a trajectory between two points lying on a horizontal plane, it is well known that the maximum distance is reached for a particle launched at an angle of 45°. For two points on a baseline making an angle β with the horizontal, the maximum range occurs for a launch angle $\alpha_{\max}$ given by

$$\tan\alpha_{\max}=\frac{(1+\sin\beta)}{\cos\beta} \tag{28}$$

with a maximum range

$$R_{\max}=\frac{2}{mg}E\frac{\cos\beta}{(1+\sin\beta)}, \tag{29}$$

yielding

$$\frac{dR}{dE}=\frac{2}{mg}=1.96\ \text{cm/neV} \tag{30}$$

for small β.

Thus we see that energy resolutions in the nanovolt region should be achievable. The idea is to use one parabolic trajectory to define the incident energy and a second trajectory to define the scattered energy. The scheme is shown in Fig. 10. The figure also shows the main principle of operation of the actual spectrometer, namely the use of mirrors to break up the parabolas so that they fit into a reasonably sized volume.

These mirrors play several other vital roles. The incident beam parabola is reflected from a moveable mirror whose position determines the distance from the image (virtual source) to the sample and hence can be used to select the incident energy. Neutrons scattered into a large range of azimuthal angles are focused onto the detector by a pair of cylindrical mirrors which are slightly elliptical, with the sample at one focus and the detector at the other. By using a multidetector one can divide the scattered neutrons into groups according to the azimuthal scattering angle and hence achieve a measure of momentum transfer resolution.

A sketch of the apparatus is shown in Fig. 11 (Steyerl *et al.*, 1983). An important and subtle feature is the focusing of the beam on the sample by the mirrors (10). This is necessary in order to provide enough incident intensity on the sample. By means of this focusing, the beam is concentrated from a width of 20 cm at the source to 5 cm at the sample, with a corresponding increase of divergence. Because of the effects of gravity, such mirrors have a strong chromatic aberration, which is compensated in this case by the energy dependence of the "reach." The actual mirror shapes needed to achieve this must be calculated numerically, and optimized so that the energy remains nearly constant over the sample area for the full range of incident energy.

An interesting property is the approximate preservation of azimuthal angles by the focusing analyzer system, so that neutrons can be detected in groups according to their azimuthal scattering angles if the cylindrical detector is divided into azimuthal chambers. Currently a two-chamber detector is installed. By changing the height of the detector, the final energy can be scanned between 420 and 440 neV for a change in height of 30 cm. With incident energies in the range of 390 to 600 neV, the calculated energy resolution is 15 neV. Figure 12 (Ebeling, 1990), shows the resolution as measured with a pure elastic scatterer (BeO powder) at the ILL, after correcting for background. The measured full width at half maximum (FWHM) is $\Delta E=15.8$ neV.

It has been pointed out by Steyerl (1978, 1992) that the usable Q range of NESSIE in its present form can be considerably broadened by measuring transmission instead of reflection. The neutrons scattered with small scattering angles are transmitted through the thin sample and then reflected from a horizontal supermirror, which is installed slightly below the sample. The elliptical analyzing mirrors then select neutrons traveling along directions with polar angles of about 40° around the vertical. As the incident neutrons arrive at an angle of $15°\pm15°$ with respect to the vertical, the Q value depends strongly on azimuthal angle. In this way measurements could be made with a minimum Q band of 0.006 ± 0.0035 Å^{-1}.

It is to be emphasized that we can only give a very sketchy outline of the many techniques employed in this instrument, and the reader is recommended to consult the original papers for a true appreciation of the many subtle ideas involved.

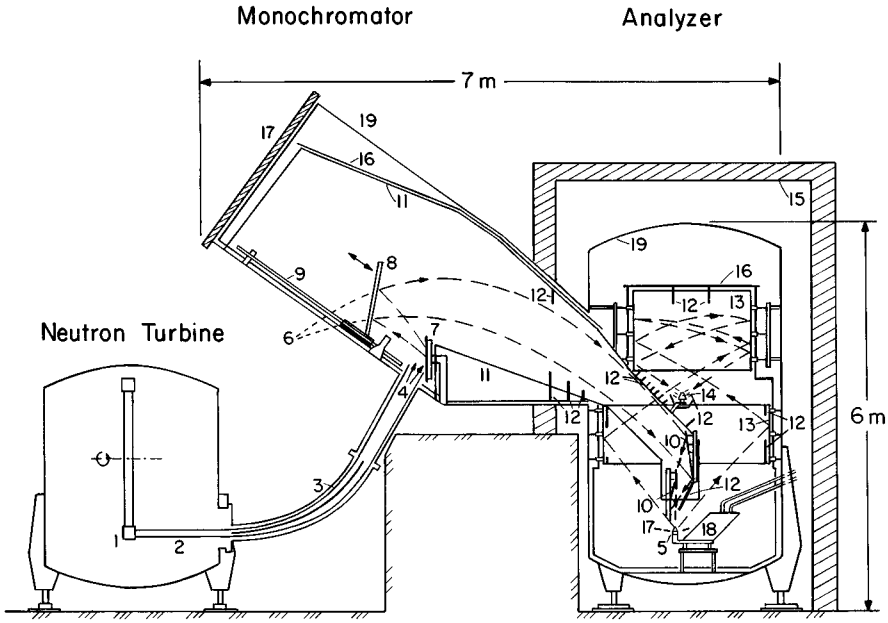

FIG. 11. Design of the gravity spectrometer NESSIE installed at the ILL, Grenoble. The ultracold neutrons are provided by the "neutron turbine." Monochromatization and energy analysis of scattered neutrons are performed by analysis of the maximum reach of the neutron flight parabolas. The spatial focusing provided by this technique is augmented, on the monochromator side, by the focusing properties of two curved mirrors (10). Also shown are: (1) blades of neutron turbine; (2,3) neutron guides; (4) source area defined by the guide exit cross section; (5) sample, surrounded by a "black absorber" (polythene); (6) virtual source; (7) first deflecting mirror; (8) monochromator mirror; (9) carriage and spindle for monochromator mirror translation; (10) focusing mirrors; (11) glass plates for lateral beam confinement; (12) beam stops; (13) cylindrical mirrors; (14) two-chamber detector with shielding and collimation elements; (15) water shielding; (16) boron containing plastic for shielding; (17) polythene shielding; (18) N_2 cryostat; (19) vacuum vessel ($p \cong 10^{-5}$ mm Hg).

In Fig. 13 we show the first reported results for high resolution UCN scattering. The line broadening observed for the dilute (0.05 g/cm^3) solution of polymer in D_2O yields a value of 13.2 ± 6.4 neV for the quasielastic linewidth (FWHM) at $Q = 0.027$ Å^{-1}. This is in agreement with a Q^3 extrapolation of previous spin-echo work at a higher Q. Although the question of the existence of a transition from the single chain ($\Delta\omega \sim Q^3$) to the many-chain regime ($\Delta\omega \sim Q^2$), expected to occur at $Q = 0.027$ Å^{-1}, could not be addressed because of complications due to multiple scattering, this result represents a stunning achievement for an installation at a reactor (Forschungs Reaktor München, FRM) with a thermal flux of 10^{13} n/cm^2/s. Comparison of Fig. 13(a) with Fig. 12 shows the improvement in counting rate achieved by moving the instrument to the Institut Laue Langevin (ILL), Grenoble.

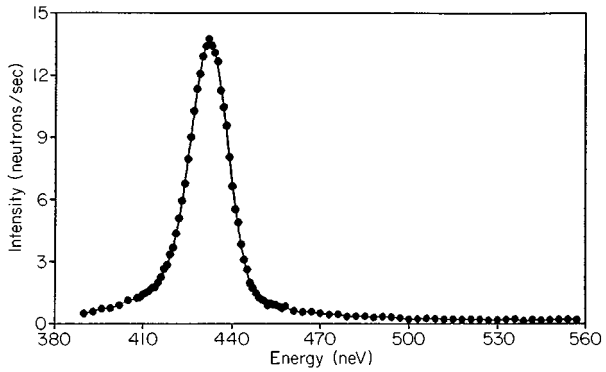

FIG. 12. Resolution curve of NESSIE. Scattering by BeO corrected for background (Ebeling, 1990).

The results of a further set of measurements at the FRM were reported by Pfeiffer *et al.* (1988). These authors measured the quasielastic scattering of neutrons by a solution of lipid bilayer in D_2O. Figure 14 shows the observed linewidth (corrected for instrument resolution) as a function of Q^2. The lowest Q point, $Q = 3 \times 10^{-2}$ Å^{-1}, was measured with ultracold neutrons, the other points with neutron spin echo. The measured UCN linewidth was found to be temperature dependent. The authors considered three possible dynamic processes to account for the measured linewidths: (i) lateral diffusion of lipid molecules, (ii) diffusion of small vesicles, and (iii) surface undulations of the bilayers. Process (ii) would require extremely small vesicles, while (iii) would result in a much broader linewidth with a Q^3 dependence; (i) provides the best explanation of the results, yielding a value for the diffusion constant D ($\sim 2 \times 10^{-7}$ cm^2 s^{-1}) in good agreement with that obtained by other techniques.

The UCN spectrometer is now installed at the ILL UCN source where the flux is about 3×10^3 times greater than at the FRM. In Fig. 15 we show the results of a

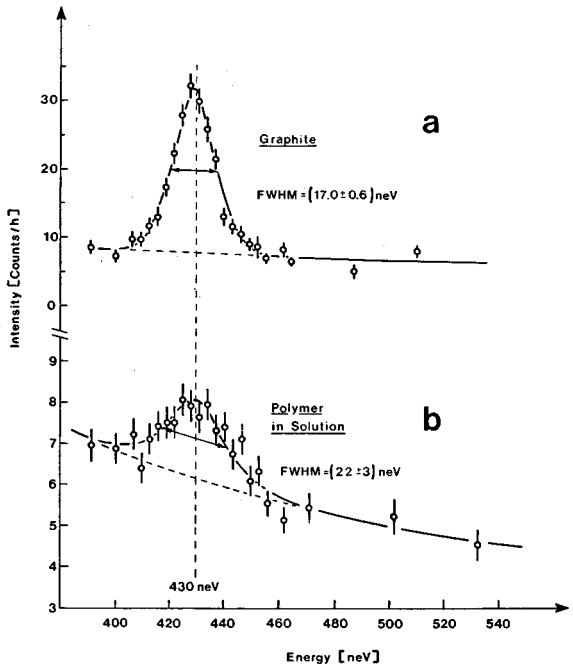

FIG. 13. The energy resolution curve of NESSIE, as measured with an elastically scattering graphite sample, is compared to the slightly broadened scattering distribution for a polydimethylsiloxane solution in deuterated benzene at 70 °C. The curves are plotted against the incident neutron energy and are centered on the analyzer energy of 430 neV (Steyerl *et al.*, 1983).

measurement which has recently been completed at the ILL: quasielastic scattering by a 1% solution of ferritin (a spherical molecule which is used for storing iron in mammals) in D_2O (Tschernitz, 1991). The figure shows a comparison between the scattering observed with the ferritin solution at 60 °C and a graphite sample used to measure the instrumental resolution. The FWHM of the quasielastic scattering is determined to be

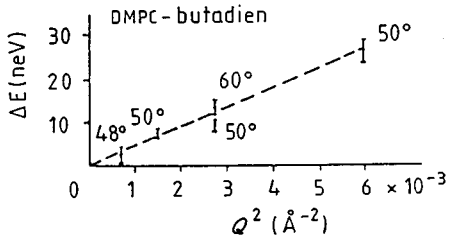

FIG. 14. Measurement of linewidth as a function of the square of the scattering vector Q. The sample is a bilayer dispersion of a 1:1 mixture of dimyristoylphosphatidylcholine (DMPC) and the photopolymerized butadiene phospholipid in pure D_2O (45% by weight). The ΔE values for $Q^2 > 3\times10^{-3}$ Å^{-2} are measured with the spin-echo spectrometer, and the value with the smallest momentum transfer with the gravity spectrometer. The measuring temperatures are given in the figure (Pfeiffer *et al.*, 1988).

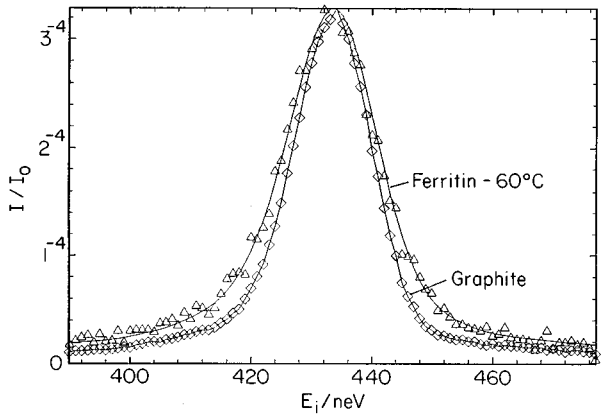

FIG. 15. Quasielastic UCN scattering by a 1% solution of ferritin in D_2O compared to the instrumental resolution of NESSIE as measured with a graphite sample (Tschernitz, 1991).

$\Delta E_{q-e} = 4.08 \pm 0.33$ neV. Measurements were made for temperatures between 10 and 60 °C. At 10 °C the measured ΔE_{q-e} is given as 1.15 ± 0.15 neV, demonstrating once again the remarkable energy resolution possible with ultracold neutrons. The Q for these measurements was 0.021 Å^{-1}, allowing for the change in neutron velocity due to the D_2O potential.

The observed temperature dependence of the quasielastic width and, thus the diffusion constant D, was in excellent agreement with that expected from the Stokes-Einstein law and published data for the viscosity.

On the basis of the results described here, we can expect that UCN scattering will begin to play a growing role in further increasing the ω-Q region available for study by neutron scattering.

V. QUASIELASTIC SCATTERING

An interesting method of studying quasielastic scattering of ultracold neutrons has been proposed by Richardson (1989) and first results have been reported by Richardson *et al.* (1991). The system makes use of a UCN storage monochromator spectrometer, shown in Fig. 16. The idea is that neutrons with total energy $> mg(H+\Delta h)$ in the storage bottle (B) will strike the absorbing roof when the storage bottle is emptied through the monochromator. Similar considerations apply to the filling of the bottle. Thus, by raising the roof while ultracold neutrons are being stored in (B), one can detect any quasielastic energy increases which may have taken place during the storage period. An interesting feature of this method is that one measures energy changes taking place after a large number ($\gtrsim 10\,000$) of wall collisions, so the sensitivity is increased spectacularly, even allowing for the fact that the neutrons undergo a random walk in velocity space.

Measurements on a storage bottle coated with a hydrogen-free fluorine-based oil called Fomblin (see Bates, 1983) yielded an rms energy change per bounce of $3.5 \pm 2.0 \times 10^{-11}$ eV, which if confirmed would repre-

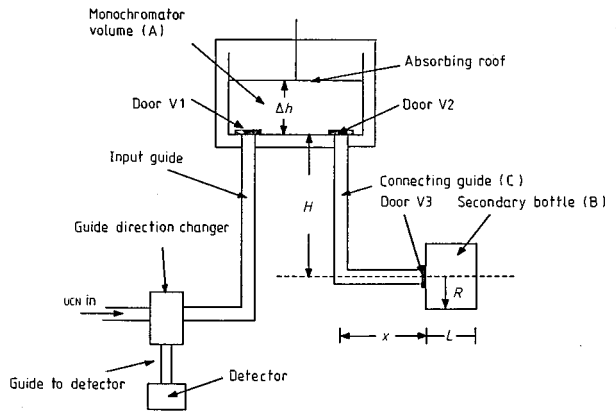

FIG. 16. Schematic diagram of the apparatus used by Richardson in searching for evidence of quasielastic heating of UCN gas within a liquid walled bottle (Richardson, 1989).

sent a truly remarkable achievement for neutron scattering (see also Golub *et al.*, 1991). With this technique, measurements could be made by inserting samples into the storage bottle whose surface characteristics would be determined by measuring without the sample present. However there is absolutely no Q information obtainable with this method, so it remains to be seen if there are any cases in which it could be useful.

VI. UPSCATTERING

We consider upscattering as being inelastic scattering in which the energy transfer is large compared to the original UCN energy. Upscattering of ultracold neutrons was first detected by Stoika *et al.* (1978), who were trying to find the cause of the anomalously short UCN storage times in material bottles. By surrounding a storage chamber with a gas-filled detector they were able to show that the rate of upscattering was consistent with the observed loss rates of stored ultracold neutrons. A detailed account of the theoretical and experimental studies of UCN storage times can be found in Golub *et al.* (1991).

Measurement of the energy spectrum of the upscattered ultracold neutrons can provide information on the scattering law $S(Q,\omega)$ for any material filling the storage vessel, or coating the walls or part of the walls. The advantages of this method might ultimately derive from the special properties of ultracold neutrons. For example, they can penetrate surfaces to a distance of $\sim$100 Å, and UCN upscattering could be used to study inelastic processes originating in this region, intermediate between the first monolayers, which are accessible to normal methods of surface physics, and the true bulk matter. To some extent this has been done in the work of Stoika *et al.* (1978). An additional advantage is that the cross sections for UCN upscattering are inherently larger than those for classical neutron scattering because of the intrinsic $1/v$ dependence of inelastic-scattering cross sections. Stored ultracold neutrons can travel distances of the order of kilometers during one storage

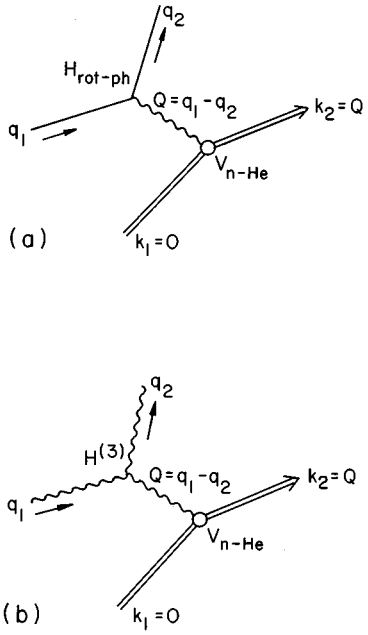

FIG. 17. Main contribution to the upscattering of ultracold neutrons in ^{4}He at low temperatures: (a) Two-roton scattering; (b) two-photon scattering.

time (in the absence of any upscattering sample), so one should be able to measure very weak scattering processes.

One disadvantage of the method is that only values of ω,Q along the "free-neutron dispersion curve"

$$\omega=\frac{\hbar Q^2}{2m}=24Q^2 \tag{31}$$

can be measured. The numerical value holds for the case where ω is measured in K and Q in Å^{-1}.

This method is being applied to the study of phonons in superfluid ^{4}He (Kilvington *et al.*, 1987; Gutsmiedl *et al.*, 1990, 1991). For coherent scattering, one-phonon absorption can only take place at the intersection of Eq. (31) with the dispersion curve, which we designate as E_c. In this case, the upscattering of ultracold neutrons at temperatures $T\lesssim 1$ K is due predominantly to one-phonon absorption ($\sim e^{-E_c/T}$, with $E_c=11.8$ K), two-phonon scattering ($\sim T^7$) and two-roton scattering ($\sim T^{3/2}e^{-E_r/T}$ with E_r=roton energy = 8.6 K). The latter two processes are shown in the diagrams in Fig. 17.

Most attention has been devoted to the two-phonon scattering which is expected to dominate at low temperatures and depends on the three-phonon interaction g_3. This interaction also determines the phonon widths, measured by techniques such as neutron spin echo or triple axis spectrometry (Mezei and Stirling, 1983; Mezei *et al.*, 1990); however, because of the narrow line widths encountered it is hoped that UCN upscattering will eventually allow measurements at lower temperatures than the more classical techniques.

Total cross sections for UCN upscattering can be measured by the effect of the upscattering on UCN stor-

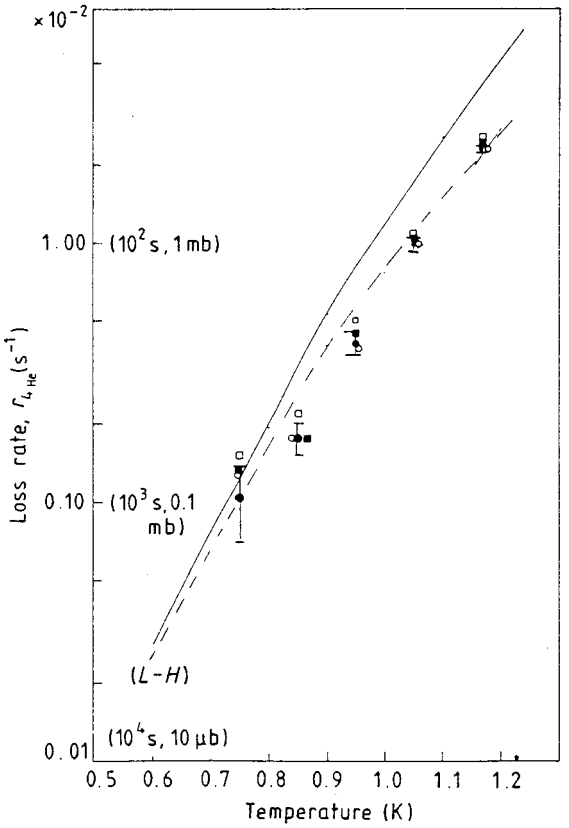

FIG. 18. Loss rate due to the interaction of ultracold neutrons with superfluid ^{4}He as a function of temperature. The numbers in brackets on the vertical scale give the corresponding storage times and total cross section (for a UCN velocity of 4.6 m s^{-1}), respectively. The broken line shows the results for the two-photon scattering process calculated using Landau's Hamiltonian (L-H). The full lines show the total loss rate. Different point styles show the results of different methods of correcting for the wall losses. Their spread indicates the uncertainties involved (Golub *et al.*, 1983).

age times. Such a program has been carried out for superfluid ^{4}He, based on the observation that, at the low temperatures involved, the wall losses are temperature independent, and that the observed large temperature dependence can be ascribed to the upscattering by the superfluid (Golub *et al.*, 1983). The results (Fig. 18) show a scattering somewhat weaker than that expected on the basis of the Landau Hamiltonian (Landau and Khalatnikov, 1949, Wilks, 1967) and three-phonon interaction as used by Maris (1977). The data of Mezei and Stirling (1983) also indicate an interaction weaker than expected on this basis and new results by Yoshiki *et al.* (1992) are also consistent with this interpretation. Recent more precise spin echo data (Mezei *et al.*, 1990) strongly reinforce this conclusion.

First measurements of the spectrum of ultracold neutrons upscattered by ^{4}He were carried out on the apparatus sketched in Fig. 19 (Gutsmiedl *et al.*, 1990, 1991). The UCN storage volume is a tube three meters long holding ten liters of liquid. The UCN valve has been machined to a thickness of 0.1 mm over 50% of its area,

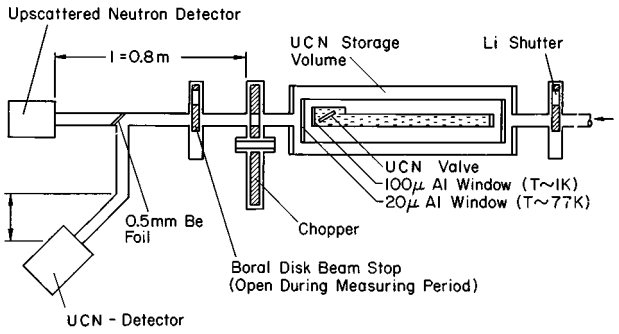

FIG. 19. Experimental setup for the measurement of the spectrum of UCN upscattered by ^{4}He (Gutsmiedl *et al.*, 1990, 1991).

so that upscattered neutrons can leave the storage volume in a direction parallel to the axis while the ultracold neutrons are held inside. The chopper is of the pseudostatistical type with 8 opening pulses out of a possible 15 per revolution. The upscattered neutrons pass through the Be foil and are detected by the in-line detector. With the chopper in the open position, UCN storage times can be measured in the usual way. Ultracold neutrons leaving the storage chamber when the UCN valve is opened are reflected from the Be foil into the UCN detector. Measurements at lower temperatures were not possible during this run because of wall losses which were larger than had been previously obtained with this apparatus. It is expected that this will be improved by suitable surface treatment (La Marche *et al.*, 1981; Mampe *et al.*, 1981). The results for the measured spectra (Fig. 20) are shifted to longer wavelengths with respect to those expected from the above theoretical considerations. Interestingly, recent spin-echo results (Fig. 21), mentioned above, also show an interaction significantly weaker than expected (Mezei *et al.*, 1990).

In these results we may be seeing the first confirmations of Woods Halley's calculation (Halley and Korth, 1990) of the three-phonon interaction. These show an extremely rich momentum dependence, with the interaction being strongest when all three phonons are nearly collinear, so one would predict an effectively weaker interaction in the UCN case than in the case of phonon width, where the conservation laws constrain the phonons to be nearly collinear. Additional work, both theoretical and experimental, is necessary to clarify the situation.

The application of the upscattering of ultracold neutrons to the study of scattering by rare-gas solids has been discussed by Achiwa (1990). This proposal is again based on the fact that coherent scattering is confined to the crossing point between the free-neutron curve and the dispersion curve. The advantage of UCN upscattering in this case is that since the energy and momentum transfer are both determined by measuring the energy of the upscattered neutrons with a polycrystalline sample, a large solid angle of scattered neutrons can be detected

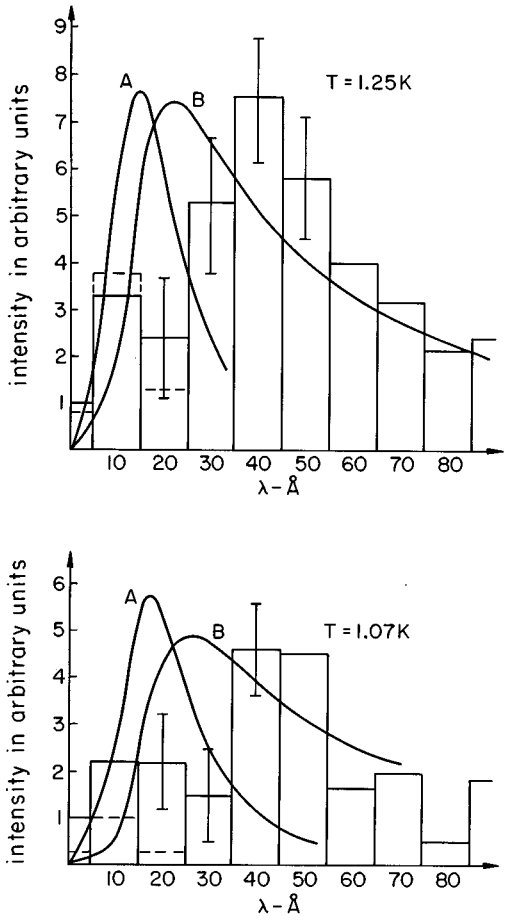

FIG. 20. Background subtracted spectra of ultracold neutrons upscattered from ^{4}He: (A) phonon-roton theory (Golub, 1979); (B) theory corrected for transmission of an ideal lossless guide; dashed histogram—expected one-phonon contribution normalized to measured spectrum (Gutsmiedl *et al.*, 1990, 1991).

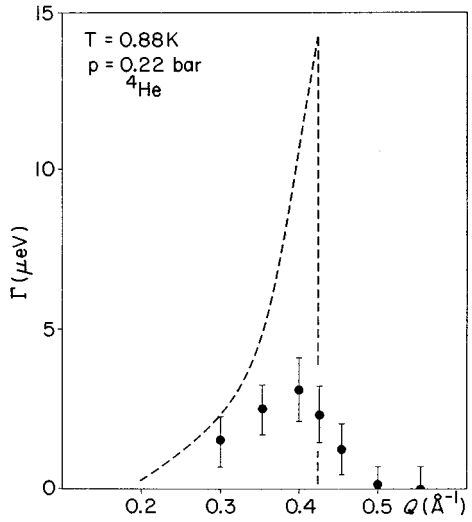

FIG. 21. Measured and calculated HWHM phonon linewidth in liquid He (Meizei *et al.*, 1990).

without broadening the resolution. Achiwa (1990) proposes to measure the energy of the upscattered neutrons by time of flight.

VII. THE FUTURE OF ULTRACOLD NEUTRON SCATTERING

It is clear from what has been said above that UCN scattering is still in its infancy. No existing instrument makes use of the full angular range allowed by the kinematics, so the full increase in intensity foreseen by Maier-Leibnitz (1966) has not yet been achieved. In spite of the great promise offered by UCN scattering the results presently available are best regarded as demonstrations of feasibility. Further progress will require improvements in instrumentation as well as more intense sources.

A. Future instrumentation

A group at Kyoto is currently working on an improved inelastic-scattering spectrometer, which uses deflection of neutron trajectories by gravity to determine the neutron's energy (Utsuro, 1983; Utsuro and Kawabata, 1983; Kawabata and Utsuro, 1992). The idea is to focus the entire solid-angle range of scattered neutrons onto a detector using systems of ellipsoidal mirrors with the source at one focus and the detector at the other, both foci being at the same height. Because of gravity, the shape of the mirrors will have to be distorted from a purely ellipsoidal shape and (this is the key point) the neutrons will be deflected to points below their geometric focus, with the deflection being a measure of the neutron energy. While it is possible in principle to use the same mirror system as a monochromator for the incident neutrons and an analyzer for the scattered neutrons (at some sacrifice of solid angle), and it is also possible to use time of flight to provide incident-energy analysis, the Kyoto group has decided to use a multilayer filter as a monochromator and as an analyzer they are using a more complex mirror system (Kawabata *et al.*, 1986) where neutrons scattered into different angular ranges are reflected from mirror sections with different foci. Thus in Fig. 22 each of the three mirror sections $M_{1,2,3}$ is focused onto a different focus, $F'_{1,2,3}$ so that on the two-dimensional position-sensitive detector D, the horizontal distribution represents Q and the vertical distribution ω. In the actual instrument (Utsuro *et al.*, 1990) the scattering angle is divided into five groups. With input velocities in the range of 4–11 m/s, selected by a multilayer filter, resolutions of $\Delta\omega \sim 25$ neV and $\Delta Q \sim 1.5\times 10^{-3}$ Å^{-1} are expected. While the amount of work put into the project is indeed impressive—the instrument will be fed from an existing supermirror turbine (Utsuro *et al.*, 1988)—it does not seem significantly different than that involved in a modern small-angle scattering instrument. At present, two of the mirror sections as well as the detector positioning mechanism and the vacuum chamber have been completed and it is hoped that preliminary tests can begin soon (Kawabata, 1995).

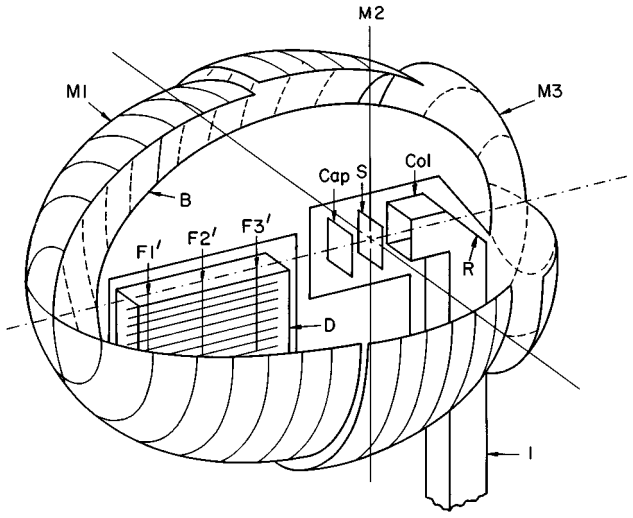

FIG. 22. Schematic design of the horizontal-type gravity analyzer. $M1$, $M2$, $M3$: neutron reflecting mirrors; $F1'$, $F2'$, $F3'$: foci of each reflecting mirror element (the other foci are at the sample position); S: sample; I: UCN feed guide tube; D: two-dimensional position sensitive detector; B: neutron absorber to avoid multiple reflections; R: reflector to deflect incident neutrons; Col: collimator for incident neutrons; Cap: transmitted beam catcher (Kawabata *et al.*, 1986).

Another possibility of a UCN spectrometer with a large range of scattering angles and reasonable Q resolution is based on the principle of neutron resonance spin echo (NRSE) (Keller *et al.*, 1990, 1995). In this scheme the sample would be surrounded by two concentric rings of coils so that the incident and scattered neutrons each pass through two resonance spin-flipper "π" coils. As a static field of 1 G in the coils (3 kHz resonant frequency) would provide 300 precessions over a 1 m flight path, only very thin foils of material will have to be placed into the beam. The relative positions of sample, coil, and incoming beam direction will have to be chosen taking the gravitational deflection into account. For example, incident neutrons traveling horizontally with a velocity of 5 m/s, will have fallen 20 cm after a 1 m flight path and will be traveling at an angle of 22° below the horizontal. For the scattered neutrons to reach their initial height after a further 1 m flight path they would have to leave the sample in a direction 22° above the horizontal. This implies a minimum Q of 6×10^{-3} Å^{-1}. The achievement of smaller Q's will require the neutrons to arrive at and leave the sample at directions closer to the horizontal, which can be achieved by proper selection of the initial flight direction and component heights. Such an instrument is still in the early discussion stage.

B. Future ultracold neutron sources

The possible development of new types of high-intensity UCN sources is another basis for a positive prognosis for UCN scattering. Existing sources, some of which use ingenious methods to extract neutrons from a reactor and present them to the user in the UCN energy range, such as the cold source—vertical extraction—neutron turbine installation at the ILL (Steyerl *et al.*, 1986) are limited by Liouville's theorem to the maximum phase-space density provided by the primary source. Of course such sources can be improved by the construction of stronger primary sources, such as the Advanced Neutron Source being designed at Oak Ridge (Hayter, 1990).

Another approach is to use a type of UCN source which is not limited to the phase-space density of the primary source, i.e., a superthermal source (Golub and Pendlebury, 1974). The idea is that UCN can be produced directly inside a storage volume by the downscattering, on a material placed into the storage vessel, of faster neutrons which can enter the closed bottle by penetration of the walls. If P is the production rate of ultracold neutrons per unit volume

$$P=\int \Phi(E)\sum (E\rightarrow E_{\mathrm{UCN}})dE, \tag{32}$$

with $\Phi(E)$ the incident flux and $\Sigma(E\rightarrow E_{\mathrm{UCN}})$ the macroscopic energy-transfer cross section for UCN production, then the steady state UCN density will be given by

$$\rho_{\mathrm{UCN}}=P\tau, \tag{33}$$

where τ is the storage time of ultracold neutrons against all loss processes, including upscattering, losses in the material, and leakage through any cracks and exit holes.

Such sources can use incident neutrons coming from all directions and hence can gain significantly in intensity by being placed closer to the primary source. In this way astonishingly large neutron densities, in comparison with existing sources, can be produced. The choice of material is, however, severely limited by the need to keep τ long in the presence of the moderator material.

Two forms of such a source have been proposed. One uses superfluid ^{4}He at temperatures around 0.7 K. ^{4}He has zero absorption, and the upscattering is limited by the fact that the scattering is purely coherent (Golub *et al.*, 1983).

The other type seeks to limit the absorption and upscattering by confining the material to a thin film on the surface of the storage bottle. Solid D_2 seems the best choice of film material. Such a source, while producing a somewhat smaller UCN density than the helium source, has two significant advantages which greatly improve its ease of installation and flexibility of use (Yu *et al.*, 1986; Golub and Böning 1983):

(1) It can operate at temperatures around 4 K, thus allowing its placement much closer to the primary source with a substantially smaller engineering effort.

(2) Since in the thin-film case P is directly proportional to the film thickness t, while $\tau\propto 1/t$, the UCN density will be independent of t, thus allowing the source to operate with shorter storage times τ without any loss of intensity. This, in turn, will allow steady-state operation

with a larger exit area (UCN source area) or a smaller volume, since the source area is limited by the requirement that the presence of the exit area should have no significant effect on τ.

VIII. CONCLUSION

Thus, while we have seen that UCN scattering has already produced some remarkable results (such as detection of quasielastic energy changes of the order of 5×10^{-11} eV, and the measurement of a quasielastic linewidth of 6 neV on a reactor with a flux of 10^{13} n/cm^2/s), we must conclude that much development work is needed before the many exciting possibilities for future work with UCN scattering become realities. However, we have every reason to expect that UCN scattering will eventually offer the highest-resolution probe at low ω and Q, thus fulfilling the original "prophecy" of Maier-Leibnitz.

ACKNOWLEDGMENTS

I would like to thank Albert Steyerl for some very helpful and encouraging discussions and Steve Lamoreaux for advice and support. I am grateful to E. Gutsmiedl and M. Tschernitz for helpful discussions of their recent work.

APPENDIX: PHASE SPACE LIMITATIONS TO INELASTIC SCATTERING EXPERIMENTS: THE ADVANTAGE OF LONGER WAVELENGTHS

In this section we give an argument, originally due to Maier-Leibnitz (1966), that for an inelastic-scattering measurement at fixed momentum transfer $\vec{Q}$ (small compared to the incoming neutron $\vec{k}$), energy transfer ω (small compared to the incoming neutron energy) and fixed $\Delta Q/Q$ and $\Delta\omega/\omega$ (the relative precisions of the Q and ω determination) one can gain intensity $\propto \lambda^2$ by going to longer incident wavelengths, provided that one makes use of the entire phase space allowed by the desired $\omega, Q, \Delta Q/Q$, and $\Delta\omega/\omega$. As a result of this we expect UCN scattering to be beneficial at relatively small values of Q and ω.

Letting $\hbar\vec{k}_f$ = final neutron momentum, $\hbar\vec{k}_i$ = initial neutron momentum, $\vec{Q}=\vec{k}_f-\vec{k}_i$, we have

$$|\vec{Q}|^2=k_f^2+k_i^2-2k_ik_f\cos\theta_s, \tag{A1}$$

where $\theta_s=\theta_f-\theta_i$ is the scattering angle. The energy transfer is $\hbar\omega=(\hbar^2/2m)(k_f^2-k_i^2)$, with m = the neutron mass. Then the fractional error in momentum transfer is

$$\frac{\Delta Q}{Q}=\frac{1}{Q^2}\left[\begin{array}{c}(k_f^2R_f)^2+(k_i^2R_i)^2+(k_ik_f\cos\theta_s)^2(R_i^2+R_f^2)+\cdots\\ \cdots+(k_ik_f\sin\theta_s)^2(\Delta\theta_s)^2\end{array}\right], \tag{A2}$$

where $R_{f,i}=(\Delta k/k)_{f,i}=$ output and input velocity resolutions and we assumed the variations in $k_{i,f}$ and θ_s are random and uncorrelated. Now

$$\Delta\theta_s=[(\Delta\theta_f)^2+(\Delta\theta_i)^2]^{1/2}, \tag{A3}$$

and the fractional error in energy transfer is

$$\frac{\Delta\omega}{\omega}=\frac{\hbar}{m}\frac{[(k_f^2R_f)^2+(k_i^2R_i)^2]^{1/2}}{\omega}. \tag{A4}$$

If we consider an experiment at a given set of values of ω and $\vec{Q}$ (assumed small), we can see how the experimental resolution of the input and output velocities and angles must vary with k_i so as to keep $\Delta Q/Q$ and $\Delta\omega/\omega$ constant:

$$R_{f,i}=(\Delta k/k)_{f,i}\propto 1/(k_{i,f})^2,$$

$$\Delta\theta_i\simeq\Delta\theta_s\propto\frac{1}{k_ik_f\sin\theta_s}\approx\frac{1}{k_i^2\sin\theta_s}, \tag{A5}$$

assuming $\omega\ll\hbar k_{f,i}^2/2m$, i.e., $k_i\simeq k_f$.

The intensity of cold neutrons (i.e., neutrons with energies small compared to the temperature) available at a target is

$$I_i\propto k_i^4R_i(\Delta\theta_i)^2, \tag{A6}$$

assuming a Maxwellian distribution of incident velocities.

Using Eq. (38), Eq. (39) becomes, for $\theta_s<1$,

$$I_i\propto\frac{1}{k_i^2\theta_s^2} \tag{A7}$$

but for a fixed $\vec{Q}$, small θ_s, and $k_i\approx k_f$, Eq. (34) gives $k_i^2\propto 1/\theta_s^2$. Therefore for a fixed Q, ω, $\Delta Q/Q$, and $\Delta\omega/\omega$ the intensity of neutrons at the target is independent of incident neutron velocity.

In an inelastic scattering experiment the counting rate I will be proportional to $I_i d\Omega_{\rm det}$, i.e.,

$$I\propto d\theta_{\rm det}d\phi_{\rm det}\sin\theta_s, \tag{A8}$$

where ϕ is the azimuthal angle. Since $d\theta_{\rm det}\approx d\theta_s$, using Eq. (38),

$$I\propto\frac{d\phi_{\rm det}}{k_i^2}. \tag{A9}$$

This means that, with the requirements of fixed Q, ω, $\Delta Q/Q$, and $\Delta\omega/\omega$, it can be more advantageous to work at longer wavelengths. This does not mean that any experiment at long wavelength will be superior to

any experiment at short wavelength, since there may be some restrictions which prevent the long wavelength system from using the entire volume of phase space allowed by the kinematic restrictions.

REFERENCES

Achiwa, N., 1990, in *Proceedings of the First Meeting on Ultra High Resolution Neutron Spectroscopy and Optics* (Kyoto University Research Reactor Institute, Kumatori), p. 54.

Bates, C., 1983, Nucl. Instrum. Methods **216**, 535.

Bée, M., 1988, *Quasi-elastic Neutron Scattering* (Adam Hilger, Bristol).

Binder, K., 1971a, Z. Naturforsch. **26a**, 432.

Binder, K., 1971b, Z. Angew. Phys. **3**, 178.

Desplanques, B., G. Gönnenwein, and W. Mampe, 1984, Eds., *Workshop on Reactor Based Fundamental Physics*, J. Phys. (Paris), Suppl. C.3 Colloque.

Dietrich, S., and R. Schack, 1987, Phys. Rev. Lett. **58**, 140.

Dilg, W., and W. Mannhart, 1973, Z. Phys. **266**, 157.

Doroshkevich, A.G., 1962, Sov. Phys. JETP **16**, 56.

Dubbers, D., P. El-Muzeini, M. Kessler, and J.C. Last, 1989, Nucl. Instrum. Methods Phys. Res. A **275**, 294.

Dubbers, D., W. Mampe, and K. Schreckenbach, 1989, Eds., *Fundamental Physics with Slow Neutrons*, Nucl. Instrum. Methods A **284**, 1.

Ebeling, H., 1990, Institut Laue-Langevin Internal Report No. 90EB07T (ILL, Grenoble).

Egelstaff, P.A., 1967, *An Introduction to the Liquid State* (Academic Press, New York).

Erozolimskii, B.G., 1975, Sov. Phys. Usp. **18**, 377.

Erozolimskii, B.G., 1989, Nucl. Instrum. Methods A **284**, 89.

Fermi, E. and L. Marshall, 1947, Phys. Rev. **71**, 666.

Fermi, E. and W.N. Zinn, 1946, Phys. Rev. **70**, 103.

Fiedeldey, H., R. Lipperheide, H. Leeb, and S.A. Sofianos, 1992, Phys. Lett. A **170**, 347.

Foldy, L.L., 1966, in *Preludes in Theoretical Physics*, edited by A. de Shalit, H. Feshbach, and L. van Hove (North-Holland, Amsterdam).

Golub, R., 1979, Phys. Lett. **72A**, 387.

Golub, R., and K. Böning, 1983, Z. Phys. B **51**, 187.

Golub, R., S. Felber, R. Gähler, and E. Gutsmiedl, 1990, Phys. Lett. A **148**, 27.

Golub, R., C. Jewell, P. Ageron, W. Mampe, B. Heckel, and A.I. Kilvington, 1983, Z. Phys. B **51**, 187.

Golub, R., and J.M. Pendlebury, 1972, Contemp. Phys. **13**, 519.

Golub, R., and J.M. Pendlebury, 1974, Phys. Lett. **50A**, 177.

Golub, R., and J.M. Pendlebury, 1979, Rep. Prog. Phys. **42**, 439.

Golub, R., D. Richardson, and S.K. Lamoreaux, 1991, *Ultra-Cold Neutrons* (Adam Hilger, Bristol).

Greene, G.L., 1986, Ed., *The Investigation of Fundamental Interactions with Cold Neutrons*, NBS Special Publication No. 711 (Natl. Bur. Stand., Washington D.C.).

Groshev, L.V., V.N. Dvoretsky, A.M. Demidov, Yu.N. Panin, V.I. Luschikov, Yu.N. Pokotilovsky, A.V. Strelkov, and F.L. Shapiro, 1971, Phys. Lett. **34B**, 293.

Gutsmiedl, E., R. Golub, and J. Butterworth, 1990, in *Excitations in Two-Dimensional and Three-Dimensional Quantum Fluids*, edited by A.F.G. Wyatt and H.J. Lauter, NATO ASI Series, Series B: Physics, Vol. 257 (Plenum, New York), p. 131.

Gutsmiedl, E., R. Golub, and J. Butterworth, 1991, Physica B **169**, 503.

Halley, J.W. and M.S. Korth, 1990, in *Excitations in Two-Dimensional and Three-Dimensional Quantum Fluids*, edited by A.F.G. Wyatt and H.J. Lauter, NATO ASI Series, Series B: Physics, Vol. 257 (Plenum, New York), p. 91.

Hauge, E.H. and J.A. Støvneng, 1989, Rev. Mod. Phys. **61**, 917.

Hayter, J., 1990, in *Proceedings of the 11th Meeting of International Collaboration on Advanced Neutron Sources* (KEK, Tsukuba, Japan), p. 890.

Herrmann, F., 1990, *Reflektrometrie mit ultrakalten Neutronen*, Diplomarbeit (Technische Universität München).

Ignatovich, V.K., 1986, *Physics of Ultra-cold Neutrons*, in Russian (Nauka, Moscow) [*The Physics of Ultra-cold Neutrons*, in English (Clarendon, Oxford, 1990)].

ILL (Institut Laue-Langevin), 1988, *Guide to Neutron Facilities*, Yellow Book (Institut Laue-Langevin, Grenoble, France).

Kawabata, Y., 1995 (private communication).

Kawabata, Y. and M. Utsuro, 1992, *Neutron Optical Devices and Applications*, SPIE J. **1738,** 454.

Kawabata, Y., M. Utsuro, and S. Okamoto, 1986, Nucl. Instrum. Methods Phys. Res. A **245**, 106.

Keller, T., R. Gähler, H. Kunze, and R. Golub, 1995, Neutron News **6**, No. 3, p. 16.

Keller, T., P. Zimmermann, R. Golub, and R. Gähler, 1990, Physica B **162**, 327.

Kilvington, A.I., R. Golub, W. Mampe, and P. Ageron, 1987, Phys. Lett. A **125**, 416.

La Marche, P.H., W.A. Lanford, and R. Golub, 1981, Nucl. Instrum. Methods **189**, 535.

Landau, L.D. and I.M. Khalatnikov, 1949, in *Collected Papers of L.D. Landau*, edited by D. ter Haar (Pergamon, New York, 1965), p. 494.

Landau, L.D. and E.M. Lifshitz, 1958, *Quantum Mechanics* (Pergamon, New York).

Lanford, W. and R. Golub, 1977, Phys. Rev. Lett. **39**, 1509.

Lekner, J., 1987, *Theory of Reflection* (Nijhoff, Dordrecht).

Lengsfeld, M., and A. Steyerl, 1977, Z. Phys. B **27**, 117.

Lermer, R., and A. Steyerl, 1976, Phys. Status Solidi A **33**, 531.

Luschikov, V.I., Y.N. Pokotilovsky, A.V. Strelkov, and F.L. Shapiro, 1968, Joint Institute for Nuclear Research, Dubna, USSR Report No. P3-4127.

Luschikov, V.I., Y.N. Pokotilovsky, A.V. Strelkov, and F.L. Shapiro, 1969, Sov. Phys. JETP Lett **9**, 23.

Maier-Leibnitz, H., 1966, Nukleonik **8**, 5.

Maier-Leibnitz, H., and T. Springer, 1963, J. Nucl. Energy **17**, 217.

Mampe, W., P. Ageron, J.C. Bates, J.M. Pendlebury, and A. Steyerl, 1989a, Nucl. Instrum. Methods A **284**, 111.

Mampe, W., P. Ageron, J.C. Bates, J.M. Pendlebury, and A. Steyerl, Phys. Rev. Lett. **63**, 593.

Mampe, W., P. Ageron, and R. Gähler, 1981, Z. Phys. B **45**, 1.

Maris, H.J., 1977, Rev. Mod. Phys. **49**, 341.

May, R.P., 1982, in *Proceedings of the Conference on the Neutron and its Applications*, edited by P. Schofield (Institute of Physics, Bristol, 1983).

Mezei, F., 1972, Z. Phys. **255**, 146.

Mezei, F., 1980, Ed., *Neutron Spin Echo* (Springer, Berlin).

Mezei, F., and P.A. Dagleish, 1977, Commun. Phys. **2**, 41.

Mezei, F., C. Lartigue, and B. Farago, 1990, in *Excitations in Two-Dimensional and Three-Dimensional Quantum Fluids*,

edited by A.F.G. Wyatt and H.J. Lauter, NATO ASI Series, Series B: Physics Vol. 257 (Plenum, New York), p. 119.
Mezei, F., and W.G. Stirling, 1983, in *25th Jubilee Conference on Helium-4*, edited by J.G.M. Armitage (World Scientific, Singapore), p. 111.
Nierhaus, K.H., R. Lietzke, R.P. May, N. Volker, H. Schulze, K. Simpson, P. Wurmbach, and H.B. Stuhrmann, 1982, Proc. Nat. Acad. Sci. USA, **80**, 2889.
Okun, L.B., 1969, Commun. Nucl. Part. Phys. **3**, 133.
Pendlebury, J. M., 1993, Annu. Rev. Nucl. Part. Sci. **43**, 687.
Penfold, J., and R.K. Thomas, 1990, J. Phys.: Condens. Matt. **2**, 1369.
Pfeiffer, W., G. Schlossbauer, W. Koll, B. Farago, A. Steyerl, and E. Sackmann, 1988, J. Phys. (Paris) **49**, 1077.
Richardson, D.J., 1989, Ph.D. thesis (University of Sussex).
Richardson, D.J., J.M. Pendlebury, P. Iaydjiev, W. Mampe, K. Green, and A.I. Kilvington, 1991, Nucl. Instrum. Meth. Phys. Res. A **308**, 568.
Scheckenhofer, H., and A. Steyerl, 1977, Phys. Rev. Lett. **39**, 1310.
Scheckenhofer, H., and A. Steyerl, 1981, Nucl. Instrum. Methods **179**, 393.
Serebrov, A. P., V.A. Mityukhlyaev, A.A. Zakharov, V.V. Nesvizhevsky, and A.G. Kharitonov, 1994, JETP Lett. **59**, 757.
Shapiro, F.L., 1968, Sov. Phys. Usp. **11**, 345.
Smith, K.F., *et al.*, 1990, Phys. Lett. B **234**, 191.
Steinhauser, K.A., A. Steyerl, H. Scheckenhofer, and S.S. Malik, 1980, Phys. Rev. Lett. **44**, 1306.
Steyerl, A., 1969, Phys. Lett. **29B**, 33.
Steyerl, A., 1977, *Neutron Physics*, Springer Tracts in Modern Physics, Vol. 80 (Springer, Berlin), pp. 57–201.
Steyerl, A., 1978, Z. Phys. B **30**, 235.
Steyerl, A., 1992 (private communication).
Steyerl, A., W. Drexel, S.S. Malik, and E. Gutsmiedl, 1988, Physica B **151**, 36.
Steyerl, A., T. Ebisawa, K.-A. Steinhauser, and Z. Utsuro, 1981, Z. Phys. B **41**, 283.
Steyerl, A., B. Gmal, K.-A. Steinhauser, N. Achiwa, and D. Richter, 1983, Z. Phys. **50**, 281.
Steyerl, A. and S.S. Malik, 1989, Nucl. Instrum. Methods A **284**, 200.
Steyerl, A., H. Nagel, F.-X. Schreiber, K.A. Steinhauser, R. Gähler, W. Gläser, P. Ageron, J.M. Astruc, W. Drexel, R. Gervais, and W. Mampe, 1986, Phys. Lett. A **116**, 347.
Steyerl, A., and H. Vonach, 1972, Z. Phys. **250**, 166.
Stoika, A.D., A.V. Strelkov, and M. Hetzelt, 1978, Z. Phys. B **29**, 349, see also Strelkov, A.V. and M. Hetzelt, 1978, Sov. Phys. JETP **47**, No. 1.
Stuhrmann, H.B. , 1982, *Proceedings of the Conference on the Neutron and its Applications* (Cambridge).
Tschernitz, M., 1991, Internal Report No. 91TS11S (Institute Laue Langevin, Grenoble, France).
Utsuro, M., 1983, Nucl. Instrum. Methods **213**, 557.
Utsuro, M., T. Ebisawa, K. Okumura, S. Shirahoma, and Y. Kawabata, 1988, Nucl. Instrum. Methods A **270**, 456.
Utsuro, M., and Y. Kawabata, 1983, Physica B **120**, 118.
Utsuro, M., Y. Kawabata, and T. Ebisawa, 1990, *Proceedings of First Meeting on Ultra-High Resolution Neutron Spectroscopy and Optics* (Kyoto University Research Reactor Institute, Kumatori), p. 41.
Vladimirskii, V.V., 1961, Sov. Phys. JETP **12**, 740.
Von Egidy, T., 1978, Ed., *Fundamental Physics with Reactor Neutrons and Neutrinos*, Conference Series No. 42 (Institute of Physics, London).
Wilks, J., 1967, *The Properties of Liquid and Solid Helium* (Clarendon, Oxford).
Yoshiki, H., K. Saka, M. Ogura, T. Kawai, Y. Masuda, T. Nakajima, T. Takayama, S. Tancha, and A. Yamaguchi, 1992, Phys. Rev. Lett. **68**, 1323.
Yu, Y-Ch., S.S. Malik, and R. Golub, 1986, Z. Phys. B **62**, 137.
Zeldovich, Ya.B., 1959, Sov. Phys. JETP **9**, 1389.